NeuroImage: Clinical 11 (2016) 30–40

Contents lists available at ScienceDirect

NeuroImage: Clinical

journal homepage: www.elsevier.com/locate/ynicl

Testing the connections within face processing circuitry in Capgras delusion with diffusion imaging tractography

Maria A. Bobes[a,*], Daylin Góngora[a], Annette Valdes[b], Yusniel Santos[a], Yanely Acosta[a], Yuriem Fernandez Garcia[c], Agustin Lage[a], Mitchell Valdés-Sosa[a]

[a]Cuban Center for Neuroscience, Havana, Cuba
[b]CENSAM, Havana, Cuba
[c]Basque Center on Cognition, Brain and Language (BCBL)

ARTICLE INFO

Article history:
Received 22 October 2015
Received in revised form 22 December 2015
Accepted 6 January 2016
Available online 7 January 2016

ABSTRACT

Although Capgras delusion (CD) patients are capable of recognizing familiar faces, they present a delusional belief that some relatives have been replaced by impostors. CD has been explained as a selective disruption of a pathway processing affective values of familiar faces. To test the integrity of connections within face processing circuitry, diffusion tensor imaging was performed in a CD patient and 10 age-matched controls. Voxel-based morphometry indicated gray matter damage in right frontal areas. Tractography was used to examine two important tracts of the face processing circuitry: the inferior fronto-occipital fasciculus (IFOF) and the inferior longitudinal (ILF). The superior longitudinal fasciculus (SLF) and commissural tracts were also assessed. CD patient did not differ from controls in the commissural fibers, or the SLF. Right and left ILF, and right IFOF were also equivalent to those of controls. However, the left IFOF was significantly reduced respect to controls, also showing a significant dissociation with the ILF, which represents a selective impairment in the fiber-tract connecting occipital and frontal areas. This suggests a possible involvement of the IFOF in affective processing of faces in typical observers and in covert recognition in some cases with prosopagnosia.

1. Introduction

Capgras delusion (CD) is a rare condition in which patients believe that their relatives have been replaced by identically looking impostors. Paradoxically, they recognize the identity of these relatives correctly, but believe that they are not who they seem to be. Ellis and Young (1990) have proposed that CD might arise from a loss of the normal affective response to familiar faces, without an impairment in face identification itself. This could create conflicting representations of the face, thus explaining the bizarre symptoms (Ellis and Lewis, 2001). In support of this hypothesis, several studies (Ellis et al., 1997; Hirstein and Ramachandran, 1997; Brighetti et al., 2007) have found that CD patients do not exhibit the increased skin conductance response (SCR) that typical subjects produce for familiar compared to unfamiliar faces (Tranel et al., 1985; Tranel and Damasio, 1985; Bobes et al., 2007). Conversely, patients with prosopagnosia may show signs of normal SCR arousal to previously familiar faces despite their inability to overtly recognize them (Bauer, 1984; Tranel et al., 1985; Bobes et al., 2004). This represents a double dissociation between overt identity recognition and covert emotional processing of familiar faces. This double dissociation has been acknowledged in a dual-route model of face processing (Ellis and Young, 1990; Bauer, 1984; Ellis and Lewis, 2001), in which one route is devoted to overt processing of personal semantic and biographic information derived from faces, whereas a parallel pathway underlies the corresponding (and optionally covert) affective responses.

Disruption of structural connectivity in the face processing circuitry has been related to prosopagnosia (Thomas et al., 2006). In a previous study (Valdes-Sosa et al., 2011), we explored the integrity of the long white matter tracts in F.E., a prosopagnosic patient that exhibited covert face recognition as well as enhanced fMRI activation for previously familiar, as compared to unfamiliar, faces. Two long-range fiber tracts, that connect key areas of the face processing system, were of special interest: The inferior fronto-occipital fasciculus (IFOF) and the inferior longitudinal fasciculus (ILF). IFOF connects the infero-lateral and dorso-lateral frontal cortex with the posterior temporal cortex (including the fusiform face area, FFA) and the occipital lobe (including the occipital face area, OFA) (Crosby et al., 1962; Catani et al., 2003). ILF connects the occipital and posterior temporal areas (including OFA and FFA) with the anterior-inferior temporal gyri and the temporal pole, and also medially to the parahippocampal gyrus and amygdala (Catani et al., 2003).

In prosopagnosic patient F.E., we found a severe impairment of the ventral portion of the ILF (in both hemispheres), whereas both IFOF

* Corresponding author at: Cuban Neurosciences Center, CNEURO, Ave 25 y 158, Cubanacan, Apartado, 12100 La Habana, Cuba.
E-mail address: antonieta@cneuro.edu.cu (M.A. Bobes).

http://dx.doi.org/10.1016/j.nicl.2016.01.006

were preserved (Valdes-Sosa et al., 2011). F.E. presented residual OFA activation that could be transmitted to the frontal areas through IFOF (which is preserved), but not to the anterior and medial temporal lobes (since the ILF is disrupted). In this sense, the disruption of ILF was implicated in the lack of overt face recognition in F.E., whereas that covert emotional processing could be mediated by his intact IFOF, which could have connected the preserved right OFA with frontal areas involved in SCR generation (Critchley et al., 2000). Thus, each of the two tracts could be hypothetically linked with a component of the dual route model mentioned above. Therefore, we hypothesized that CD patient would present the inverse pattern found in F.E.: an intact ILF with a damaged IFOF. Here we employed DTI-tractography to test this proposal in a CD patient, that presented a lack of SCR affective response to familiar faces.

Previously, Bauer (1984) had proposed that, after initial analysis in visual areas, affective processing of familiar faces could involve a "dorsal" route via the superior temporal sulcus that would then project through the superior longitudinal fasciculus (SLF) to the frontal lobes (Bauer, 1984). A lesion to this hypothetical route could contribute to a lack of affective processing in CD, hence the SLF integrity was also explore.

An alternative neurological theory of CD pathogenesis states that CD originates from a disconnection between the two hemispheres, leaving in each representations that does not interact with the other, therefore generating a sense of discordant familiarity (Joseph, 1986) see Barton (2003) for review. According with this theory, we could expect to find some damage in the fiber tracks connecting the left and right hemispheres. In order to examine this hypothesis, the commissural tracts: forceps major (FMj) and forceps minor (FMi) were also explored in the present study.

It is important to clarify that a lack of SCR to familiar faces is not sufficient to produce the CD, since, i.e. fronto-ventromedial lesions produce the same dissociation between autonomic response and overt recognition (Tranel et al., 1995) but do not cause the CD. This has been previously discussed by Ellis and Lewis (2001), locating the abnormality at different places of the face recognition model for CD and fronto-ventromedial lesioned patients (but see the debate around this in Breen et al., 2001; Lewis and Ellis, 2001). More recently, Coltheart (2007, 2009, 2010) has postulated that lack of affective processing (autonomic symptom) is not sufficient to bring about the Capgras delusion, and that a second factor is needed, which could be an impairment in the belief evaluation process. This second factor seems to be associated to damage in right dorsolateral prefrontal cortex (Coltheart, 2007), which has been found in CD (Devinsky, 2009). Therefore, we also explore gray matter integrity in our CD patient using voxel base morphometry (VBM) with the hypothesis that some damage will be found in the right frontal area.

To eliminate the possibility that our results were unreliable, we repeated the CD patient's neuroimaging study twice, with a six-month interval between the two recording sessions. Moreover, voxel base morphometry (VBM) was used for a quantitative estimation of possible gray and white matter tissue damage (based in both the T1 image and fractional anisotropy from the DTI). Since this is a single case study, it is important to eliminate any cause other than the patient's lesion as an explanation for his tractography results. The fiber counts in any of the patient's tracts could be reduced due to idiosyncratic noise, or simply by a difference in the degree of head movement respect to controls (Yendiki et al., 2013). Consequently, the white matter VBM results were used to project any lesions found in the patient onto the DTI images from matched control cases. This allowed us to estimate the effects the lesions would have had (if present) on fiber tracts in the controls. This simulation permitted us to test if the fiber tract anomalies in the patient were completely explainable by his localized brain damage (see discussion in (Valdes-Sosa et al., 2011)). In other words, we tested if the white matter lesions per se were capable of generating any tractography anomalies in the patient.

2. Methods and materials

2.1. Patient description

Patient J.R. (male) was referred for psychiatric, neurological and neuropsychological evaluation because of a psychotic episode four years before this study. He was diagnosed with Delusional Ideas Disorder following the DSM IV criteria by a psychiatrist who confirmed the patient's CD. Toxic habits of alcohol abuse and other psychiatric symptoms (depression and anxiety) were ascertained in the initial evaluation, as well as a family history of dementia and alcohol abuse.

Capgras delusion (CD) started at about 12 months after this initial referral. Family members reported that J.R. started to believe that a policeman had replaced his daughter as an impostor. J.R. was strongly convinced that his daughter, although identical in every way to the real one, was a different person. Over the following months and years this symptom persisted, with an extension to other relatives (sons and grandsons).

At the time of this study, J.R. was 71 years old. He is right handed, had low school qualification, and an intelligence quotient (IQ) of 104 as estimated with WAIS-R (Silverstein, 1982). He presented a Minimental State Examination (Folstein et al., 1975) score of 23, and a Clinical Dementia Rating (Hughes et al., 1982) score of 1, indicating mild cognitive impairment. His clinical and neurological examination evinced a moderate hearing loss in the left ear and the presence of abnormal slow movement and tremors. An electroencephalographic (EEG) study revealed abnormal amplitude in the background activity in the left hemisphere, where fronto-temporal paroxysmal activity was also detected. A clinical MRI of the brain showed diffuse cerebral atrophy. The patient's history and the clinical findings suggested the diagnosis of degenerative dementia (fronto-temporal or Lewy bodies), although the nosological classification remains uncertain.

On follow-up examinations, a progressive decline of cognitive functions was documented. In particular, significant fluctuations and reduction in alertness and more prominent deficits in working memory and executive functions were observed (see Supplementary material, Table ST1). The total scores (23 of a maximum of 30 points) on the Mini-Mental State Examination (MMSE) and WAIS-R Estimated IQ (104) are both due to significantly poorer executive functioning performance. MMSE points were mainly lost on the attentional component (attention subscore) and the WAIS-R Estimated IQ points were mainly lost on the non-verbal problem-solving skills, influenced by visuospatial, planning, executive and motor skills. Non-verbal block design performance was poorer as opposed to on the verbal vocabulary performance (see Supplementary material, Table ST1).

J.R. had been treated with various antipsychotic drugs over the 4 years before the study. At the time of the present study he was taking trifluoperazine (25 mg/day) and fluphenazine (55 mg/day). A neuropsychological evaluation revealed that J.R. had mild to moderate cognitive impairment. On follow-up examinations, a progressive decline of cognitive functions was documented. In particular, significant fluctuations in alertness, and more prominent deficits in working memory and executive functions were observed. J.R. was disoriented in time and his verbal communication became difficult with very slow spontaneous speech and dysprosody, as well as frequent anomie.

At the time of this study J.R. reported no problems relating to face recognition or identification, but the Capgras syndrome persisted. Neuropsychological examination at the time of the present study is showed in Supplementary material (Table ST1).

2.2. Control group

Ten right-handed healthy male subjects matched in age with the patient (mean age = 70.2) participated as controls in the study. All of these subjects had at least a high-school degree. Participants were screened to exclude neurological, psychiatric, and systemic diseases.

All participants (including J.R.) were recruited as volunteers after giving informed consent. The experimental protocols were approved by the Ethics Committee of Cuban Center for Neuroscience.

2.3. Skin conductance response

SCRs were measured in J.R. using the same procedure described before (Bobes et al., 2004, 2007). The experimental task was presented on a sVGA monitor and consisted of passive viewing of 37 faces. These consisted of 24 unfamiliar faces randomly mixed with 13 familiar faces, the latter selected among close relatives and acquaintances as suggested before (Lucchelli and Spinnler, 2007). Each stimulus was presented for 2 s followed by more than 20 s of inter-stimulus intervals.

Electrodermal activity was recorded using Ag/AgCl electrodes attached to the palmar surface of the proximal phalanx of left index and middle fingers. The signal was registered via a skin conductance processing unit (GSR-2100, Nihon Kohden) to a channel of a MEDICID III/E system. The filtered analog output of the SCR was displayed online and recorded digitally (100 Hz sample rate), in synchrony with the onset of the face and following the procedure described before (Bobes et al., 2007).

The results in a control group (similar in age to J.R.) as well as in a prosopagnosic patient were described in Bobes et al. (2004). As described in previous studies, larger SCRs were obtained to familiar than to unfamiliar faces in normal controls.

2.4. Magnetic resonance imaging study

The MRI study was repeated twice with a period of six months between the two recordings sessions, which were carried out using the same equipment and parameters. These two set of images were analyzed independently in order to estimate the reliability of the findings.

Image acquisition: A Siemens 1.5T Magnetom Symphony system with a standard birdcage head coil for signal transmission/reception (Siemens, Erlangen, Germany) was used. A MPRAGE T1-weighted structural image ($1 \times 1 \times 1$ mm resolution) was acquired with the following parameters: echo time (TE) = 3930 ms, repetition time (TR) = 3000 ms, flip angle = 15° and field of view (FOV) = $256 \times 256 \times 160$ mm. This yielded 160 contiguous 1 mm thick slices in a sagittal orientation. Diffusion weighted images (DWI) were undertaken along twelve independent directions, in 50 slices of 3 mm, with 2 mm × 2 mm in plane resolution, and a diffusion weighting b value of 1200 s/mm^2. The following parameters were used: acquisition matrix size = 128×128, TE = 160 ms, TR = 7000 ms, flip angle = 90° and FOV = 256×256 mm. A T2 reference image (b0 image) with no diffusion weighting was also obtained (b = 0 s/mm^2). The aforementioned acquisition was repeated 5 times to improve signal to noise ratio (SNR). Magnitude and phase difference images of a T2 gradient echo field mapping sequence were acquired with TE = 7.71 ms and 12.47 ms in order to improve EPI quality. Although the scanner sequence performs an automatic eddy current correction, an affine 3D mutual normalized information-based registration method was used to remove remaining distortions (Studholme et al., 1998). The DW-MRI images were corrected from EPI distortions using the SPM FieldMap toolbox. T1-weighted 3D anatomical image was registered to the b = 0 image using a normalized mutual information method (Studholme et al., 1998). After correction for image distortions due to the diffusion gradients, the diffusion tensor and the fractional anisotropy (FA) were determined in each voxel (Basser and Pierpaoli, 1996).

2.5. Voxel-based morphometry (VBM)

VBM analysis was performed over gray matter concentration and FA maps. First, each participant's T1 scan was corrected for inhomogeneities, spatially normalized to MNI-space, and segmented into gray matter (GM), white matter (WM), and cerebrospinal fluid, using the unified procedure in SPM5. The unnormalized T1 image was also rigidly co-registered with the b0 image using a mutual information cost function (Collignon et al., 1995). The FA maps then underwent an affine transformation into the original T1 space, and were subsequently transformed into the Montreal Neurological Institute (MNI) space using the warping parameters estimated for the T1 image. The segmented/normalized gray tissue and the normalized FA maps were smoothed with 12 and 8 mm isotropic Gaussian kernels respectively. For each type of image, a one tailed t-test was performed to identify those voxels that presented significantly lower GM concentration or FA in J.R. than in the ten age-matched control subjects. To adjust for multiple comparisons, significance levels for the test were set using false discovery rates (FDR) of 0.05, calculated from the estimation of an empirical null distribution for each type of image (Schwartzman et al., 2009). The anatomical lesions were referred to the AAL atlas (Tzourio-Mazoyer et al., 2002) for GM concentration, and to the WMPM atlas (Mori et al., 2008) for the FA results. Additionally, the locations of GM anatomical lesion were compared with the functional regions of interest (ROIs) selective for face defined by Julian et al. (2012), downloaded from http://web.mit.edu/bcs/nklab/GSS.shtml.

2.6. Deterministic tractography

Three-dimensional reconstruction of the tracts was performed using the Fiber Assignment by Continuous Tracking (FACT) method (Mori et al., 1999) as implemented in DTI_tool toolbox (www.uniklinik-reiburg.de/mr/live/arbeitsgruppen/diffusion_en.html) using the default settings. The diffusion tensor images (DTI) were movement-, eddy-current-, and distortion-corrected. DTI analysis was performed in each subject's native space. Start and ending masks were selected with an FA and trace thresholds of 0.1 and 0.0016 respectively. A turning angle threshold of 53.1° and minimum fiber length of 5 voxels were used. Tracking was performed from all voxels inside the brain (brute-force approach), and then assigned to the specific tracts using multi-ROI approach (Wakana et al., 2007). To test our a priori hypothesis the following white matter tracts were studied: IFOF, ILF (the ventral part), and SLF in each hemisphere as well as FMj and FMi of the corpus callosum. (Additionally, other major association tracts were reconstructed, see Supplementary material).

ROIs defined in previous publications were used as the basis for the tract definitions (Wakana et al., 2007). All ROI were first manually traced on the MNI152 average brain, and then transformed to each subject's DTI native space. This was done via inverse transformations of the following series of mappings used for: 1) Realignment of a high resolution anatomical T1 image, initially coregistered to DTI B0 image, to the standard position on the AC-PC plane; 2) Normalization (jointly with segmentation) of the T1 image to MNI space using the procedure from SPM5. After each ROI mapped to DTI native space it was then inspected visually and corrected with deletions or additions of voxels if necessary. The ROIs was selected as described previously (Wakana et al., 2007), except those for IFOF and ILF, which were slightly modified as described in our previous article (Valdes-Sosa et al., 2011) See Supplementary material (Table ST1) for description.

The streamline count was quantified for each tract and used as the dependent measurement in the analysis. Other measures were obtained for each tract: number of intersected voxels (NIV), defined as the number of voxels which were traversed by at least one of the streamline in the tract, as well as the average of FA and the average of the mean diffusivity (MD) and radial diffusivity (RD) within each tract.

2.7. Lesion effect simulations

In an attempt to replicate “in silico” the findings for J.R., “virtual lesions” were inflicted on the control subject DTI data. This allowed us to control for the influence of patient specific nuisance variables such as imaging noise, and head movement in the tractography data of J.R.

which would not be present in the controls. For this simulation, the voxels occupied by the patient's lesions (as identified by the VBM analysis over the FA images) were projected into each subject's native space (using in each case the respective parameters obtained for normalization into MNI space). In each subject, we eliminated all fibers traced by the FACT that fell within the virtual lesion territory. This allowed us to submit streamlines counts from DTI to a repeated-measure analysis of variance (2 by 2 ANOVA) with lesion (before and after simulated lesion) and tract (IFOF and ILF) as factors. The counts entered into the ANOVA were first logarithmically transformed to reduce skewedness.

2.8. CD patient/control-group comparisons

A modified t-test developed for single-case studies (Crawford and Garthwaite, 2002) was used for all univariate patient/control-group comparisons (Crawford and Garthwaite, 2002), in order to examine the presence of a classical dissociation between the IFOF and IFL counts in the patient with respect to the control-group. Operationally, the definition of classical dissociation requires that the patient should be impaired in one tract, but within the normal limits for the other tract. Furthermore, the difference between tract counts in the patient should be larger than those found in the control group, taking into account the correlation between both tract counts (Crawford et al., 2003). The logarithm of streamline counts was used in this analysis. The significance level of comparisons was set at 0.00125 (a p of 0.05 with the Bonferroni correction).

3. Results

3.1. Skin conductance response

J.R. did not exhibit differential autonomic responses to familiar and unfamiliar faces (mean = 0.013 μS, SD = 0.0067 μS for familiar faces and mean = 0.0127 μS, SD = 0.0068 μS for unfamiliar faces, $t(34) = -0.122$, ns). We removed from the analysis one face of acquaintances, which J.R. could not recognize after the experiment.

3.2. VBM

VBM identified the voxels that were significantly lower either in GM concentration or in FA when the CD patient was compared with the age-

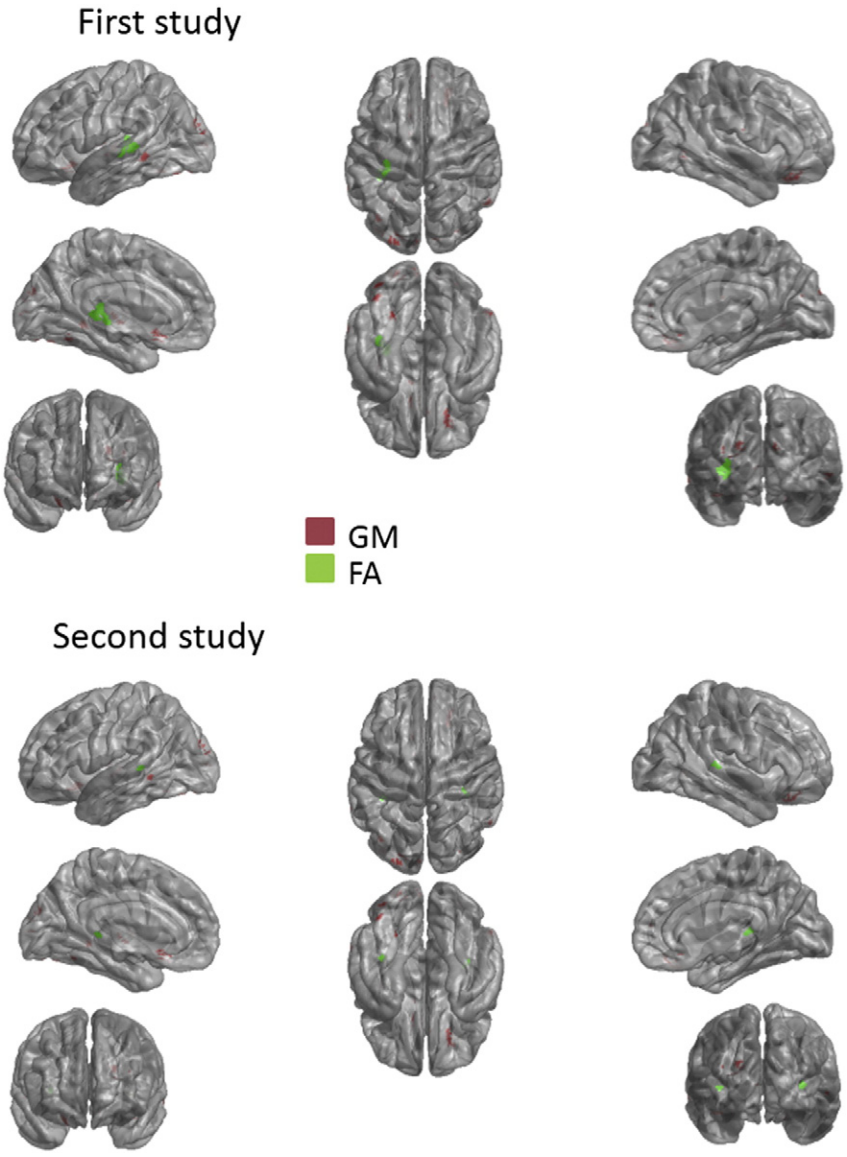

Fig. 1. Voxel based morphometry A) Voxel based morphometry of GM and FA in patient J.R. for the first and second study. A tridimensional rendering of damaged voxels (FDR threshold, q = 0.05) overlaid on J.R.'s transparent cortical surface for GM (in red) and for FA (in green). In this and subsequent figures cortical surfaces were extracted with the Freesurfer package; and plotted with custom software.

matched controls. Three-dimensional renderings of the VBM results for GM concentration and FA in the first and second studies are presented in Fig. 1, which were highly replicable over time. GM lesions were concentrated mainly in the frontal lobes, with larger clusters located at the right frontal inferior orbital, right frontal superior orbital, right frontal middle orbital and the left olfactory gyri (Table 1A). These damaged areas did not overlap the territories of the functional face selective areas (less than 1% of overlapping), except for the right OFA, where the lesion occupied the 2.8% of the ROI, but this result was not reliable since it was only obtained in the second study (Table 1B). The FA analysis evinced white matter abnormalities that were reliably present in the left hemisphere, overlapping partially the retrolenticular part of the internal capsule and the posterior thalamic radiation. In the right hemisphere a small locus of WM damage was present in the retrolenticular part of the internal capsule, but this result was only seen in the second study. The anomalies reflected in the VBM were not clearly detectable by visual inspection in the T1 scan.

3.3. Tractography analysis

The total streamline count (bruteforce) in J.R. was similar to that found in normal controls (first study: $t(9) = 0.1$, ns; second study: $t(9) = 1.29$, ns), see Table 2.

3.3.1. Commissural tracts

The reconstructed FMj and FMi from both hemispheres are shown in Fig. 2A, for a typical control subject and for J.R. Both commissural tracts in the patient were similar to those found in the control (Fig. 2A). No difference was found in the streamline counts between J.R. and controls (Table 2, Fig. 2B), neither for FMj (first study: $t(9) = 0.28$, ns; second study: $t(9) = 0.94$, ns) nor for FMi (first study: $t(9) = 0.54$, ns; second study: $t(9) = 0.23$, ns).

3.3.2. SLF

In patient J.R., the left and right SLF tracts were similar to those found in the controls (comparison with a typical control is shown in Fig. 3A). No difference was found in the streamline counts between J.R. and controls (Table 2, Fig. 3B), neither for the left hemisphere (first study: $t(9) = 0.16$, ns; second study: $t(9) = 0.06$, ns), nor for the right hemisphere (first study: $t(9) = 0.55$, ns; second study: $t(9) = 0.04$, ns).

3.3.3. IFOF and ILF

The reconstructed IFOF and ILF from both hemispheres for J.R. and a typical control are shown in Fig. 4A. In J.R. both tracts were present, but the left IFOF seems to be reduced in size compared with the control. Equivalent results were obtained in the first and second studies. The streamline count analysis is shown in Fig. 4B (note that confidence intervals for single case test are shaded in blue light) and Table 2. In J.R., the streamline count for the left IFOF was significantly smaller than in the age-matched controls (first study: $t(9) = 5.27$, $p < 0.0002$; second study: $t(9) = 4.21$, $p < 0.001$), whereas the count for the right IFOF was not significantly different from that seen in controls (first study: $t(9) = 0.25$, ns; second study: $t(9) = 0.7$, ns). The streamline counts in both hemispheres for the ILF were equivalent for J.R. and controls (first study: left: $t(9) = 0.91$, ns; right: $t(9) = 0.5$, ns; second study: left: $t(9) = 0.22$, ns; right: $t(9) = 1.9$, ns). This dissociation between IFOF

Table 1
Gray matter regions showing significant differences between patient J.R. and typical controls ($p < 0.05$, FDR corrected).

A) Referred to the AAL atlas (Tzourio-Mazoyer et al., 2002).

Region	First study					Second study				
	x	y	z	# of voxels damaged	%	x	y	z	# of voxels damaged	%
Right hemisphere										
Frontal sup orb R	20	26	−22	39	3.91	20	26	−22	35	3.51
Frontal mid orb R	24	28	−22	18	1.77	24	32	−20	11	1.08
Frontal med orb R	8	26	−14	7	0.82	8	26	−14	4	0.47
Frontal inf orb R	28	28	−20	10	0.59	26	30	−20	2	0.12
Rectus R	8	28	−16	4	0.54	8	28	−16	3	0.40
Temporal mid R						58	−60	−2	15	0.34
Left hemisphere										
Olfactory L	−6	18	−14	6	2.14	−8	14	−14	14	5.00
Occipital sup L	−20	−92	22	19	1.39	−20	−92	20	41	3.00
Rectus L	−8	18	−16	7	0.82	−10	22	−18	19	2.23
Calcarine L	−8	−96	0	15	0.66	−6	−96	2	10	0.44
Occipital mid L	−22	−92	20	10	0.31	−26	−92	16	54	1.65
Frontal med orb L	−6	22	−14	2	0.28	−6	22	−14	2	0.28
Caudate L	−6	16	−10	1	0.10	−6	14	−12	6	0.62
Cuneus R						12	−92	22	10	0.70
Temporal mid L						−66	−46	−8	37	0.75

B) Referred to the functional regions of interest (ROIs) selective for faces (Julian et al., 2012, http://web.mit.edu/bcs/nklab/GSS.shtml).

ROI/hemisphere	First study			Second study	
	ROI size (# of voxels)	# of voxels damaged	%	# of voxels damaged	%
pSTS R	2505	0	–	6	0.23
FFA R	1019	0	–		
V1 bil	2461	9	0.3	16	0.65
FFA L	531	0	–		
OFA L	790	0	–		
Anterior cingulate bil	1351	0	–	1	0.07
pSTS L	844	0	–		
Middle orbitofrontal bil	700	1	0.14		
Precentral R	365	0	–		
Temporal middle R	183	0	–		
OFA R	211	0	–	6	2.8
Frontal inferior orbital R	149	0	–	0	
Poseriort cingulate bil	166	0	–		

L, left hemisphere; R, right hemisphere; x y z MNI coordinates of cluster centroid; % of damage in each structure; bil, bilateral % of damage in each structure.

Table 2
Streamline count values in the controls and J.R. patient. Data are presented as mean values and standard deviations. T and p-value resulted from the statistical comparison for single case studies.

	Brute-force	Fmj	Fmn	SLF left	SLF right	IFOF left	IFOF right	ILF left	ILF right
mean	65,000	93.90	323.60	312.40	344.90	194.90	332.10	218.40	238.60
SD	8710	87.05	247.66	169.17	222.24	98.19	175.32	117.55	150.69
J.R. Study 1	60,036	81.00	383.00	245.00	412.00	7.00	197.00	352.00	285.00
T	−0.10	0.29	0.54	−0.17	0.55	**−5.28**	−0.25	0.92	0.48
p	0.46	0.39	0.30	0.44	0.30	**0.00025**	0.40	0.19	0.32
J.R. Study 2	49,398	18.00	216.00	282.00	284.00	14.00	120.00	157.00	33.00
T	1.30	−0.94	−0.23	0.07	−0.04	**−4.21**	−0.72	−0.23	−1.92
p	0.11	0.18	0.41	0.47	0.48	**0.00113**	0.24	0.41	0.04

Bold p-values represent those that survived the Bonferroni correction of $p < 0.00125$.
FMj: forceps major; FMi: forceps minor; SLF: superior longitudinal fasciculus; ILF: inferior longitudinal fasciculus; IFOF: inferior fronto-occipital fasciculus.

and ILF damage was confirmed by a test for differential impairments in the left hemispheres (first study: $t(9) = 6.1$, $p < 0.0001$; second study: $t(9) = 4.1$, $p < 0.001$). The same test was not significant in the right hemisphere (first study: $t(9) = 0.76$, ns; second study: $t(9) = 0.46$, ns).

3.4. Lesion simulation

The effects of simulating the patient FA lesion on the control DTI data is also shown in Fig. 4B (gray symbols). The mean streamline count for the left IFOF after the virtual lesion in the controls is smaller than the count without the lesion, and the latter is similar in magnitude to the actual count obtained in patient J.R. Also, the streamline counts for the right IFOF and for both ILFs were not different before and after the virtual lesion. This was confirmed in a 2 by 2 ANOVA. The left hemisphere control data showed a significant effect of simulated lesion ($F(1,9) = 24,6$, $p < p > 0.00074$) and tract ($F(1,9) = 13,4$, $p < 0.0005$), and importantly a highly significant interaction of tract and simulated lesion ($F(1,9) = 22,4$, $p < 0.001$), due to the greater reduction of IFOF- compared to ILF-counts. Hence, the lesion simulations (base only on FA VBM anomalies) affected the streamlines in controls, reproducing J.R.'s pattern of streamline counts.

The analysis of other measures obtained from these tracts confirms the previous results (Table 3). No differences were found in NIV, FA, MD and RD for the following tracts: FMj, FMi, and left and right SLF

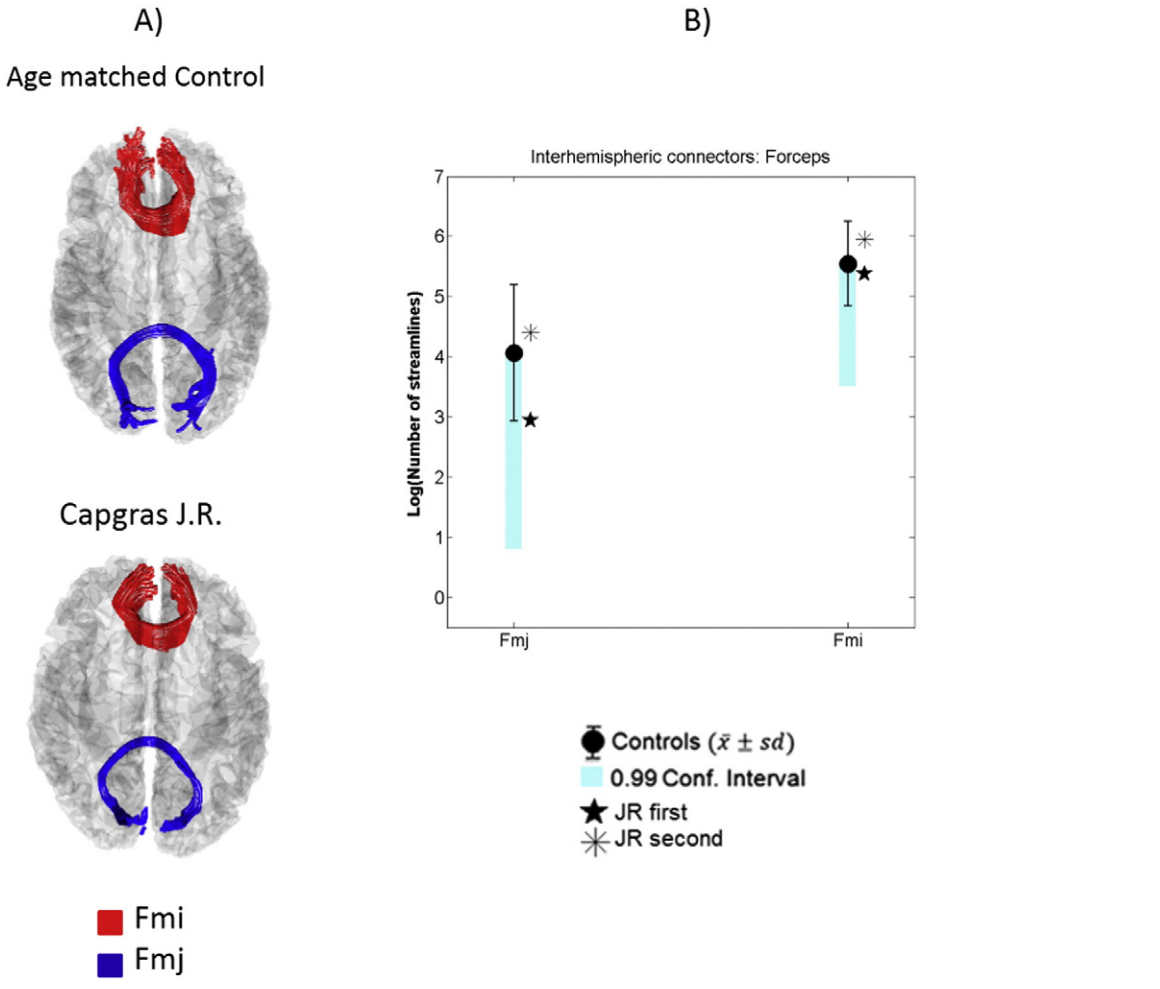

Fig. 2. Results of deterministic tractography of the FMj and FMi tracts. A) Tridimensional representation in a control subject and patient J.R. on their individual transparent cortical surfaces (upper view). B) Logarithm of streamline counts for patient J.R. and controls. The blue bars represent the 99% confidence-intervals for single-cases.

(Table 3). However, the left IFOF NIV was significantly smaller in J.R. than in the age-matched controls (first study: $t(9) = 5.5$, $p < 0.00018$; second study: $t(9) = 6.0$, $p < 0{,}0001$), whereas the NIV for the right IFOF and left and right ILF was not significantly different from that seen in controls, which confirms the dissociation between IFOF and ILF damage. No difference in FA and MD were found in left and right IFOF neither in the ILF.

The same analysis for the other association tracts showed no significant differences in streamline counts nor other measures (see Supplementary material).

4. Discussion

No difference in SCR response between familiar (i.e. the patient's relatives) and unfamiliar faces was found in J.R., consistent with previous results in other CD patients (Ellis et al., 1997; Hirstein and Ramachandran, 1997; Ellis and Lewis, 2001). This reduced autonomic reactivity to familiar faces has been referred as hypoemotionality (Bauer, 1984). A lack of normal affective reactivity to faces of family members is seen as a critical component of CD.

Previous studies have provided evidence that CD can be associated to gross brain damage (Edelstyn and Oyebode, 1999; Huang et al., 1999; Breen et al., 2000; Josephs, 2007). Bilateral or right-hemisphere abnormalities, particularly in the frontal region and in the temporal and/or parietal lobes, have been reported with visual inspection of MRI or CAT scans (Lewis, 1987; Hirstein and Ramachandran, 1997; Edelstyn et al., 2001; Breen et al., 2002; Devinsky, 2009; Luca et al., 2013). The importance of the right frontal lobes in many different forms of delusion, including CD has been previously discussed (Coltheart, 2007; Devinsky, 2009). Our results using VBM also implicated larger clusters in the right frontal orbital gyri, and in the left olfactory gyrus. Since the localization of reported gray matter lesions varies greatly across different studies, even when VBM has been used (Jedidi et al., 2015), the need for further studies is warranted. In this study we analyzed the impact of the patient GM lesion on the nodes of the face sensitive neural areas by calculating the overlap between the VBM identified lesions and previously published functional ROIs (Julian et al., 2012). We found that the nodes of the face processing circuitry were essentially unaffected, since only a minimal and non-replicable overlap with OFA was observed. A recent fMRI study (Thiel et al., 2014) reported lack of activation for familiar faces in a CD patient. This patient presented a GM lesion in right prefrontal cortex that did not include areas of the face extended system like middle orbitofrontal cortex (mOFC), posterior cingulate and STS. In the same study, they reported impaired functional connectivity between these areas and frontal lobe in the left hemisphere.

VBM of FA has not been previously reported for white matter in CD patients. Clear signs of white matter damage were found with VBM in J.R., with reduced FA values compared to controls in areas around the retrolenticular part of internal capsule and posterior thalamic radiation in the left hemisphere. With visual inspection of MRI, Edelstyn et al. (2001) reported a patient with right hemisphere subcortical white-matter pathology in the frontal and parietal lobes and a diagnosis of vascular cognitive impairment. Another study (Luca et al., 2013) reported a patient with lesions in the frontal subcortical white matter bilaterally. It is difficult to compare these previous studies with ours.

Tractography showed that, (with the exception of the left IFOF) all of the tracts explored in our patient (i.e. ILF, SLF, FMj and FMi), were similar in streamline counts, as well as in the other measures obtained in each track (FA, MD, RD and NIV), to the age-matched controls. Contrariwise, the left IFOF was reduced in NIV and fiber counts were significantly below the values measured in controls. These results in J.R. were

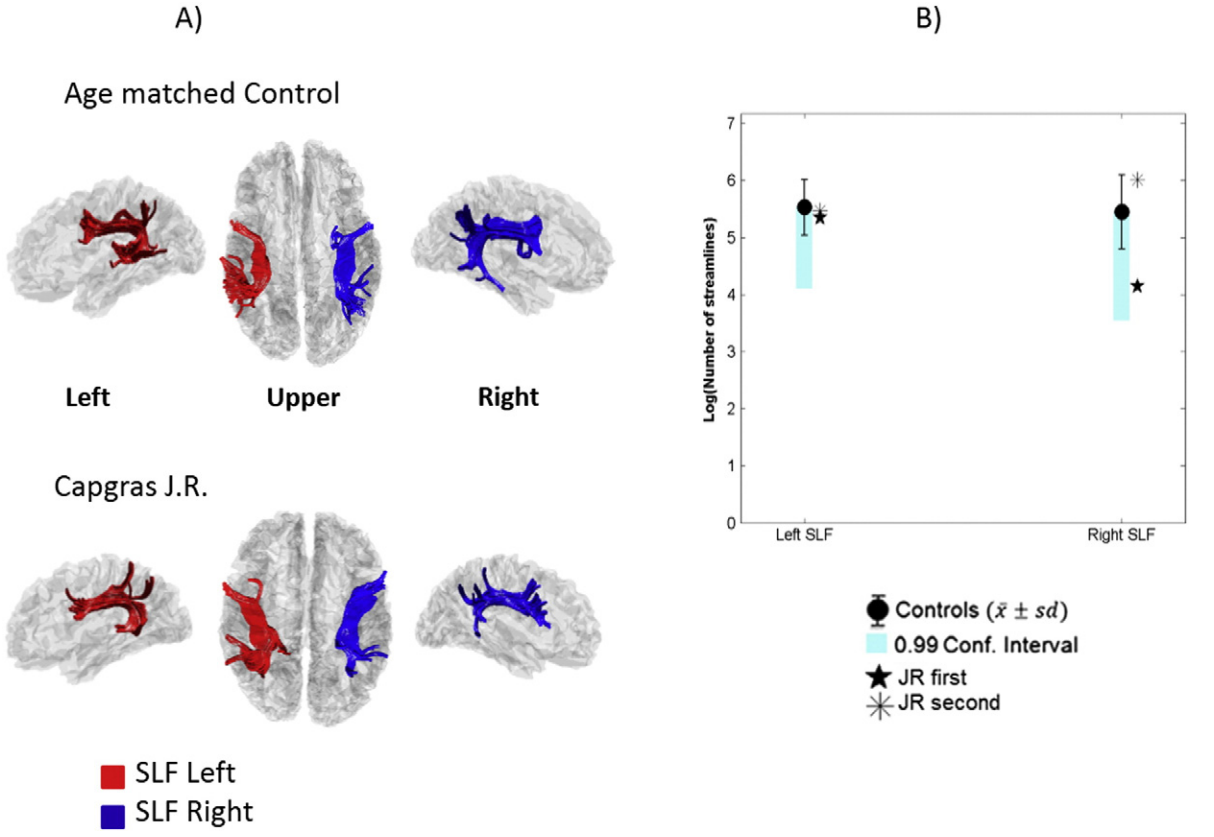

Fig. 3. Results of deterministic tractography of the left and right SLF tracts. A) Tridimensional representation in a control subject and patient J.R. on their individual transparent cortical surfaces. B) Logarithm of streamline counts for patient J.R. and controls. The blue bars represent the 99% confidence-intervals for single-cases.

replicated in two different studies carried out six months apart. The same pattern of fiber counts for all tracts was reproduced in the controls data when the streamlines in the space occupied by the patient's VBM lesions were "knocked out". This indicates that the WM lesions identified with VBM were capable of explaining the tractography results in J.R., and that his results were not attributable to idiosyncratic artifacts, noise, or head motion selectively affecting the left IFOF territory in his data.

These results allowed us to exclude other neuroanatomical accounts of CD in our patient. The commissural tracts were preserved in J.R., with streamline counts of FMj and FMi that did not differ from the controls. Note that the posterior FMj connects the temporal-occipital cortices, and the anterior FMi connects the amygdala and temporal pole (Wakana et al., 2007; Catani and Thiebaut de, 2008). This means that the commissural connections of territories containing the main face processing regions were examined in the present study. This precludes abnormal interhemispheric connections as an explanation for CD in our patient, a hypothesis previously advanced for this disorder (Joseph, 1986; Horikawa et al., 2006) and for other delusional states (Filteau et al., 1991; Woodruff et al., 1995; Wang et al., 2008; Görgülü et al., 2010). On the other hand, the intact STS (not implicated by the gray matter VBM) and SLF (with a normal fiber tally) also discount a damaged 'dorsal' route for affective processing, at least as originally

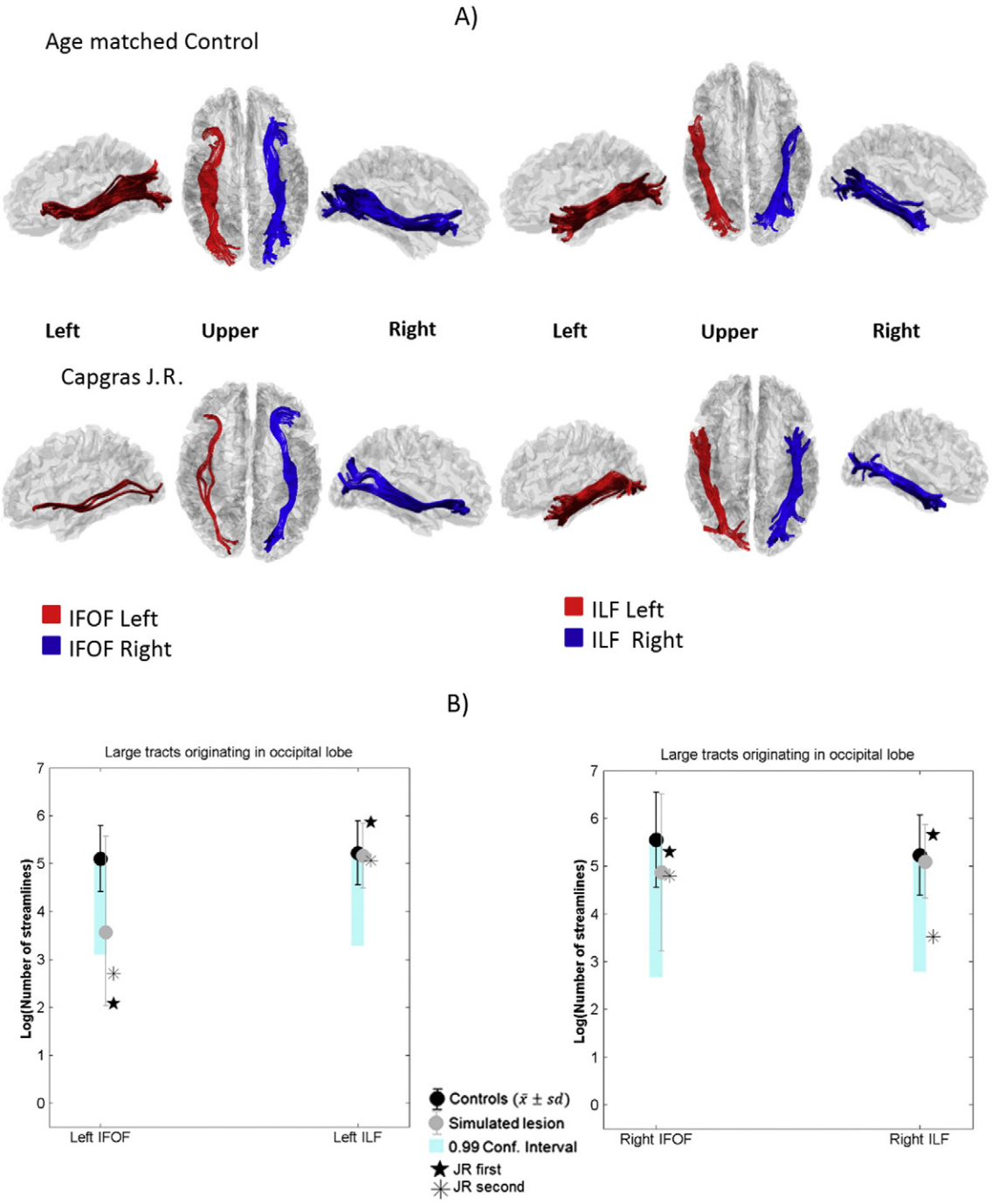

Fig. 4. Results of deterministic tractography of the IFOF and the ILF tracts. A) Tridimensional representation of the IFOF and the ILF in a control subject and patient J.R. on their individual transparent cortical surface. B) Logarithm of streamline counts for J.R. and controls. The blue bars represent the 99% confidence-intervals for single-cases. Grey symbols represent the controls means and standard deviations before and after simulated lesions.

Table 3
Other diffusion tensor measurements values in the controls and J.R. patient. Data of number of intersected voxels (NIV), fractional anisotropy (FA); mean diffusivity (MD) and radial diffusivity (RD) are presented as mean values and standard deviations. T and p-value resulted from the statistical comparison for single case studies.

	Fmj	Fmn	SLF left	SLF right	IFOF left	IFOF right	ILF left	ILF right
NIV								
Mean	530,500	1251.50	1408.20	1346.50	1051.50	1278.80	908,300	976,100
SD	427,872	637,237	893,839	556,218	389,653	529,912	327,690	366,521
J.R. Study 1	553,000	1387.00	1451.00	1127.000	312,000	980,000	1020.00	1053.00
T	0.42461	0.39765	0.31287	−0.25018	**−5.5035**	−0.20467	0.42624	0.32992
p	0.34055	0.35008	0.38075	0.40403	**0.00019**	0.42119	0.33997	0.37450
J.R. Study 2	271.00	782,000	654,000	1348.00	275,000	876,000	537,000	285,000
T	−0.0572	−0.5848	−1.0389	0.17809	**−6.0462**	−0.37305	−1.04454	−2.49903
p	0.47781	0.28651	0.16296	0.43130	**0.00010**	0.35887	0.16174	0.01696
FA								
Mean	0.35220	0.35207	0.32380	0.32562	0.36581	0.36002	0.35711	0.33576
SD	0.10563	0.03845	0.02101	0.02013	0.01941	0.03073	0.02175	0.02766
J.R. Study 1	0.40092	0.33772	0.31283	0.31965	0.38985	0.34930	0.33230	0.33098
T	0.43973	−0.35574	−0.49764	−0.28251	1.80123	−0.33282	−1.08765	−0.16475
p	0.33525	0.36511	0.31533	0.39197	0.05259	0.37345	0.15251	0.43639
J.R. Study 2	0.48336	0.32864	0.31592	0.31425	0.33143	0.32196	0.32129	−0.80198
T	1.18388	−0.58093	−0.35768	−0.53864	−1.51914	−1.18118	−1.57001	−1.47504
p	0.13339	0.28777	0.36441	0.30160	0.08152	0.13390	0.07543	0.22161
MD								
Mean	0.00085	0.00084	0.00079	0.00079	0.00085	0.00085	0.00085	0.00084
SD	0.00008	0.00006	0.00005	0.00005	0.00005	0.00005	0.00005	0.00006
J.R. Study 1	0.00081	0.00078	0.00075	0.00073	0.00086	0.00084	0.00084	0.00080
T	−0.41923	−1.06944	−0.68128	−1.02683	0.14530	−0.24514	−0.22210	−0.68726
p	0.34244	0.15636	0.25642	0.16565	0.44384	0.40592	0.41460	0.25462
J.R. Study 2	0.00085	0.00084	0.00077	0.00077	0.00090	0.00089	0.00083	0.00081
T	0.02290	−0.07373	−0.37018	−0.27458	1.03829	0.70049	−0.34274	−0.50377
p	0.49112	0.47142	0.35990	0.39492	0.16311	0.25066	0.36983	0.31326
RD								
Mean	0.00121	0.00118	0.00107	0.00106	0.00121	0.00120	0.00120	0.00116
SD	0.00019	0.00005	0.00006	0.00006	0.00007	0.00006	0.00007	0.00007
J.R. Study 1	0.00121	0.00108	0.00101	0.00098	0.00123	0.00116	0.00116	0.00110
T	0.01900	−1.79636	−1.00013	−1.37131	0.77740	−0.54829	−0.47540	−0.80494
p	0.49263	0.05300	0.17169	0.10175	0.22843	0.29841	0.32291	0.22080
J.R. Study 2	0.00136	0.00115	0.00104	0.00104	0.00122	0.00120	0.00114	0.00107
T	0.75479	−0.58543	−0.51047	−0.45503	0.65440	−0.00542	−0.76997	−1.18454
p	0.23483	0.28632	0.31100	0.32993	0.26461	0.49790	0.23053	0.13327

Bold p-values represent those that survived the Bonferroni correction of $p < 0.00125$.
FMj: forceps major; FMi: forceps minor; SLF: superior longitudinal fasciculus; ILF: inferior longitudinal fasciculus; IFOF: inferior fronto-occipital fasciculus.

proposed (Bauer, 1984) which implicated a connection from temporal–parietal to frontal cortices. It is important to note that our results do not speak to the validity of other cognitive explanations proposed for CD (Breen et al., 2000; Lucchelli and Spinnler, 2007, 2008).

In patient J.R. the left IFOF was disrupted whereas the connections with the temporal lobe via the ILF survived. Thus, connections between occipital and frontal lobes were affected, with no damage (as ascertained with VBM) to face specific functional areas. This damage could have caused a weakening of links between OFA/FFA, and areas like the lateral orbitofrontal cortex (OFC) and the insula, that have been implicated in generating emotion from face identity (Gobbini and Haxby, 2007; Bobes et al., 2013). Possibly indirect links from OFA/FFA to the medial OFC could also have been affected (Kringelbach and Rolls, 2004). This is precisely the pathway we proposed for covert recognition in prosopagnosia, based on our previous neuroimaging study of prosopagnosic patient F.E. (Valdes-Sosa et al., 2011). This idea is indirectly supported by a study with a large sample of patients, that found that emotional expression recognition can be impaired by unilateral damage in IFOF (Philippi et al., 2009).

It is interesting to note that the left IFOF reduction in NIV and streamline count was not accompanied by changes in FA, MD or RD. This could be mean that the microstructural characteristics of the residual tract remained normal, and that the main deficit is associated with tract extension. Moreover, as it has been pointing out before (Jones et al., 2013), tracking takes place only where the FA is large (in our case above 0.1), which introduces a bias in the measurements. Thus, for example the mean FA could have been calculated only on the core of less affected fibers in a partially damaged tract. In turn, streamline counts as an index of tract integrity can also be problematic, since other factors such as image noise and other features of the pathway (curvature, length, width, myelination), can affect this measure (Jones et al., 2013). However, the simulation described above, showed that the knocking out tracks in the patient's lesion space, but in a set of normal images, leads in the latter to the same streamline reduction found in the former. Thus the reduced streamline counts in J.R., are more closely linked to the anatomy of his lesion than to any uncontrolled idiosyncratic variable in his recording.

Some additional issues require discussion. The most important referred to the lateralization of the IFOF damage. We found disruption of connectivity in J.R. only in the left hemisphere, which is discrepant with the right hemisphere or the bilateral brain damage most frequently reported in CD. However, the lesions we detected here were not evident on visual inspection of the MRI scan. Since previous studies have not explored WM integrity using DWI nor VBM, they may have missed subtle left hemisphere anomalies. Strong support to this came from a recent fMRI study in which left functional connectivity was impaired in a CD patient (Thiel et al., 2014), which is congruent with our results. Another study found left hemisphere damage in CD using SPECT (Peña-Salazar et al., 2014). Positive emotion and approach behavioral tendencies have been associated with function of the left hemisphere (Davidson et al., 1990; Davidson, 1992; Davidson and Irwin, 1999). Data from several studies using different methods such as fMRI, VBM, electrophysiology and patient lesion support the importance of left frontal areas for processing positive affective stimuli. Also, data for

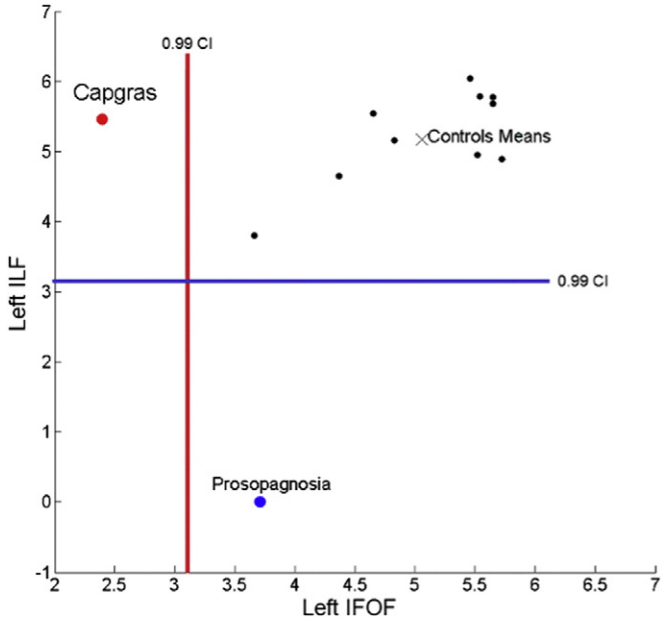

Fig. 5. Single case analysis of the IFL/IFOF streamline counts in the left hemisphere. In black: each individual control, in red CD patient J.R. (mean of the two studies) and in blue prospagnosic patient F.E: All were represented according to the logarithm of streamline counts for the left IFL and left IFOF. Vertical and horizontal lines indicates the lower 99% confidence-intervals for single-cases in each axe.

cell recording in monkeys confirmed that neuronal activity in cells in the lateral prefrontal cortex (LPFC) and dorsolateral prefrontal cortex (DLPFC) are modulated by reward value of the stimuli (Watanabe, 1996). Left lateralization of the deficit in our findings is compatible with the left positively valence hemisphere hypothesis of emotion (Davidson, 1992). If Capgras delusion resulted from lack of affective processing of familiar faces, we must expected the involvement of the left hemisphere in its processing, since familiar faces are highly positive and approaching stimuli.

Another issue deserving discussion is the variability in anatomical damage location and basal pathology in CD patients (Huang et al., 1999; Josephs, 2007). This heterogeneity reaffirms the need for further studies including more than one case in order to generalize our findings in patient J.R. However, it is possible that the same syndrome could arise from lesions to different sites in a widespread brain network involved in affective processing of faces. Another critical point would be to consider that the probable diagnosis of patient J.R. is fronto-temporal dementia (FTD), which is accompanied by morphological changes in frontal lobe. Several studies have compared fiber tract integrity in fronto-temporal dementia with normal controls (Borroni et al., 2007; Matsuo et al., 2008; Zhang et al., 2009; Whitwell et al., 2010). For all these studies widespread damage has been found in most major long fasciculi, e.g. FA reduction in SLF, IFL and IFOF in both hemispheres (Borroni et al., 2007), and Fmi, ILF and CST (Whitwell et al., 2010). Our study suggest that when the damage is selective, sparing the ILF but impairing at least the left IFOF, then more specific syndromes such as CD, can arise. A study comparing FTD patient with and without CD would be very interesting.

Fig. 5 shows a comparison of streamline counts for IFOF and ILF, restricted to the left cerebral hemisphere, for the CD patient J.R. and the prosopagnosic patient F.E. (data from Valdes-Sosa et al., 2011, was reanalyzed). As described above, in J.R. the left IFOF count is below the single case confidence interval, whereas his left IFL count is within normal limits. In contrast, prosopagnosic patient F.E. presents the inverse pattern, with the ILF count below (and the IFOF within) the confidence interval for controls. Moreover, the IFL and IFOF counts are very different in the two patients. We therefore clearly demonstrate a double dissociation in the left hemisphere between the impairments of IFOF and ILF when J.R. and F.E. are considered together.

Our results provide a neuroanatomical grounding of those models of face processing that emphasize the deficit in covert familiarity responses with intact overt person as a critical aspect of Capgras delusion (Ellis and Young, 1990, Breen et al., 2000a, 2000b; Ellis and Lewis, 2001). They posited the idea that the CD and prosopagnosia might be cognitive mirror images of one another. This means that prosopagnosia could result from partial damage to the core face system supporting overt recognition, with a residual functional capacity for unconscious affective processing. In contrast, CD might arise when the reverse pattern of damage occurs, that is, an intact overt recognition system that is partially disconnected from an impaired covert system. We suggest that these two subsystems include either ILF or IFOF respectively as major highways connecting their corresponding cortical areas.

A similar claim had been anticipated by Fox et al. (2008), who analyzed the premises needed for postulating a disconnection in the face processing circuitry. They postulated that disconnection of the core processing system areas with the subsystem mediating affective responses would result in intact familiarity of faces, as well as intact access to other person information through faces, without the appropriate emotional response. This would result in the subjective experience of a face that 'looks' familiar but does not 'feel' familiar.

Our results are also congruent with the two-factor framework of delusions proposed by Coltheart (2007) and Coltheart (2010). According with this theory the presence of CD requires a first factor that prompts the delusion and a second factor, which is an additional deficit in delusion evaluation processing (which may be executive control processes for monitoring and evaluating the contents of delusion), Coltheart (2010). In our CD case, there is a first deficit in affective reactivity in face recognition (lack of SCR) that is probably caused by the left IFOF impairment. The second deficit in our case could be associated to the presence of GM damage in the frontal lobes.

In conclusion, our data demonstrates that gray matter right frontal damage and a selective impairment in the left IFOF in a case of Capgras delusion. This association tract connects the core faces areas (OFA/FFA) with the frontal areas of the extended face recognition system that are involved in processing affective values of familiar faces (Gobbini and Haxby, 2007). Possibly this pathway could be involved in unconscious processing of faces in typical observers and in some cases of prosopagnosia with covert face recognition.

Acknowledgments

Special thanks are extended to J.R. and control cases for their participation in the study. The authors thank the Center of Medical and Surgical Research in Havana for its help in imaging, and the Cuban Human Brain Mapping Project for providing neuroinformatics support.

Appendix A. Supplementary data

Supplementary data to this article can be found online at http://dx.doi.org/10.1016/j.nicl.2016.01.006.

References

Barton, J.J., 2003. Disorders of face perception and recognition. Neurol. Clin. 21, 521–548.
Basser, P.J., Pierpaoli, C., 1996. Microstructural and physiological features of tissues elucidated by quantitative-diffusion-tensor MRI. J Magn Reson. B 111, 209–219.
Bauer, R.M., 1984. Autonomic recognition of names and faces in prosopagnosia: a neuropsychological application of the Guilty Knowledge Test. Neuropsychologia 22, 457–469.
Bobes, M.A., Lopera, F., Comas, L.D., Galan, L., Carbonell, F., Bringas, M.L., et al., 2004. Brain potentials reflect residual face processing in a case of prosopagnosia. Cogn Neuropsychol. 21, 691–718.
Bobes, M.A., Quinonez, I., Perez, J., Leon, I., Valdes-Sosa, M., 2007. Brain potentials reflect access to visual and emotional memories for faces. Biol. Psychol. 75, 146–153.
Bobes, M.A., Lage, C.A., Quinones, I., Garcia, L., Valdes-Sosa, M., 2013. Timing and tuning for familiarity of cortical responses to faces. PLoS One 8, e76100.

Borroni, B., Brambati, S.M., Agosti, C., Gipponi, S., Bellelli, G., Gasparotti, R., et al., 2007. Evidence of white matter changes on diffusion tensor imaging in frontotemporal dementia. Arch. Neurol. 64, 246–251.
Breen, N., Caine, D., Coltheart, M., Hendy, J., Roberts, C., 2000a. Towards an understanding of delusions of misidentification: four case studies. Mind Lang. 15, 74–110.
Breen, N., Caine, D., Coltheart, M., 2000b. Models of face recognition and delusional misidentification: a critical review. Cogn Neuropsychol. 17, 55–71.
Breen, N., Coltheart, M., Cane, D., 2001. A two-way window on face recognition. Trends Cogn. Sci. 5, 234–235.
Breen, N., Caine, D., Coltheart, M., 2002. The role of affect and reasoning in a patient with a delusion of misidentification. Cogn Neuropsychiatry 7, 113–137.
Brighetti, G., Bonifacci, P., Borlimi, R., Ottaviani, C., 2007. "Far from the heart far from the eye": evidence from the Capgras delusion. Cogn Neuropsychiatry 12, 189–197.
Catani, M., Thiebaut de, S.M., 2008. A diffusion tensor imaging tractography atlas for virtual in vivo dissections. Cortex 44, 1105–1132.
Catani, M., Jones, D.K., Donato, R., Ffytche, D.H., 2003. Occipito-temporal connections in the human brain. Brain 126, 2093–2107.
Collignon, A., Maes, F., Delaere, D., Vandermeulen, D., Suetens, P., Marchal, G., 1995. Automated multi-modality image registration based on information theory. In: Bizais, Y., Barillot, C., Di Paola, R. (Eds.), Information Processing in Medical Imaging. Kluwer Academic Publishers, Dordrecht, pp. 263–274.
Coltheart, M., 2007. The 33rd Sir Frederick Bartlett Lecture: cognitive neuropsychiatry and delusional belief. Q. J. Exp. Psychol. 60, 1041–1062.
Coltheart, M., 2009. Delusions and misbeliefs. Behav. Brain Sci. 32, 517.
Coltheart, M., 2010. The neuropsychology of delusions. Ann. N. Y. Acad. Sci. 1191, 16–26.
Crawford, J.R., Garthwaite, P.H., 2002. Investigation of the single case in neuropsychology: confidence limits on the abnormality of test scores and test score differences. Neuropsychologia 40, 1196–1208.
Crawford, J.R., Garthwaite, P.H., Gray, C.D., 2003. Wanted: fully operational definitions of dissociations in single-case studies. Cortex 39, 357–370.
Critchley, H.D., Elliott, R., Mathias, C.J., Dolan, R.J., 2000. Neural activity relating to generation and representation of galvanic skin conductance responses: a functional magnetic resonance imaging study. J. Neurosci. 20, 3033–3040.
Crosby, E.C., Humphrey, T., Lauer, E.W., 1962. Correlative Anatomy of the Nervous System Macmillan New York.
Davidson, R.J., 1992. Anterior cerebral asymmetry and the nature of emotion. Brain Cogn. 20, 125–151.
Davidson, R.J., Irwin, W., 1999. The functional neuroanatomy of emotion and affective style. Trends Cogn. Sci. 3, 11–21.
Davidson, R.J., Ekman, P., Saron, C.D., Senulis, J.A., Friesen, W.V., 1990. Approach-withdrawal and cerebral asymmetry: emotional expression and brain physiology: I. J. Pers. Soc. Psychol. 58, 330–341.
Devinsky, O., 2009. Delusional misidentifications and duplications: right brain lesions, left brain delusions. Neurology 72, 80–87.
Edelstyn, N.M., Oyebode, F., 1999. A review of the phenomenology and cognitive neuropsychological origins of the Capgras syndrome. Int J Geriatr.Psychiatry 14, 48–59.
Edelstyn, N.M., Oyebode, F., Barrett, K., 2001. The delusions of Capgras and intermetamorphosis in a patient with right-hemisphere white-matter pathology. Psychopathology 34, 299–304.
Ellis, H.D., Lewis, M.B., 2001. Capgras delusion: a window on face recognition. Trends Cogn. Sci. 5, 149–156.
Ellis, H.D., Young, A.W., 1990. Accounting for delusional misidentifications. Br. J. Psychiatry 157, 239–248.
Ellis, H.D., Young, A.W., Quayle, A.H., De Pauw, K.W., 1997. Reduced autonomic responses to faces in Capgras delusion. Proc. Biol. Sci. 264, 1085–1092.
Filteau, M.J., Pourcher, E., Bouchard, R.H., Baruch, P., Mathieu, J., Bedard, F., et al., 1991. Corpus callosum agenesis and psychosis in Andermann syndrome. Arch. Neurol. 48, 1275–1280.
Folstein, M.F., Folstein, S.E., McHugh, P.R., 1975. "Mini-mental state". A practical method for grading the cognitive state of patients for the clinician. J. Psychiatr. Res. 12, 189–198.
Fox, C.J., Iaria, G., Barton, J.J., 2008. Disconnection in prosopagnosia and face processing. Cortex 44, 996–1009.
Gobbini, M.I., Haxby, J.V., 2007. Neural systems for recognition of familiar faces. Neuropsychologia 45, 32–41.
Görgülü, Y., Alparslan, S.C., Uygur, N., 2010. Corpus callosum atrophy and psychosis: a case report. Düsünen Adam: The Journal of Psychiatry and Neurological Sciences 23, 137–141.
Hirstein, W., Ramachandran, V.S., 1997. Capgras syndrome: a novel probe for understanding the neural representation of the identity and familiarity of persons. Proc. Biol. Sci. 264, 437–444.
Horikawa, H., Monji, A., Sasaki, M., Maekawa, T., Onitsuka, T., Nitazaka, Y., et al., 2006. Different SPECT findings before and after Capgras' syndrome in interictal psychosis. Epilepsy Behav. 9, 189–192.
Huang, T.L., Liu, C.Y., Yang, Y.Y., 1999. Capgras syndrome: analysis of nine cases. Psychiatry Clin. Neurosci. 53, 455–459.
Hughes, C.P., Berg, L., Danziger, W.L., Coben, L.A., Martin, R.L., 1982. A new clinical scale for the staging of dementia. Br. J. Psychiatry 140, 566–572.
Jedidi, H., Daury, N., Capa, R., Bahri, M.A., Collette, F., Feyers, D., et al., 2015. Brain metabolic dysfunction in Capgras delusion during Alzheimer's disease: A positron emission tomography study. Am. J. Alzheimer Dis. Other Demen. 30, 699–706.
Jones, D.K., Knosche, T.R., Turner, R., 2013. White matter integrity, fiber count, and other fallacies: the do's and don'ts of diffusion MRI. NeuroImage 73, 239–254.
Joseph, A.B., 1986. Focal central nervous system abnormalities in patients with misidentification syndromes. Bibl. Psychiatr. 68-79.
Josephs, K.A., 2007. Capgras syndrome and its relationship to neurodegenerative disease. Arch. Neurol. 64, 1762–1766.
Julian, J.B., Fedorenko, E., Webster, J., Kanwisher, N., 2012. An algorithmic method for functionally defining regions of interest in the ventral visual pathway. NeuroImage 60, 2357–2364.
Kringelbach, M.L., Rolls, E.T., 2004. The functional neuroanatomy of the human orbitofrontal cortex: evidence from neuroimaging and neuropsychology. Prog. Neurobiol. 72, 341–372.
Lewis, S.W., 1987. Brain imaging in a case of Capgras' syndrome. Br. J. Psychiatry 150, 117–121.
Lewis, M.B., Ellis, H.D., 2001. A two-way window on face recognition: reply to Breen et al. Trends Cogn. Sci. 5, 235.
Luca, M., Bordone, A., Luca, A., Patti, A., Sortino, G., Calandra, C., 2013. Clinical features and imaging findings in a case of Capgras syndrome. Neuropsychiatr. Dis. Treat. 9, 1095–1099.
Lucchelli, F., Spinnler, H., 2007. The case of lost Wilma: a clinical report of Capgras delusion. Neurol. Sci. 28, 188–195.
Lucchelli, F., Spinnler, H., 2008. A reappraisal of person recognition and identification. Cortex 44, 230–237.
Matsuo, K., Mizuno, T., Yamada, K., Akazawa, K., Kasai, T., Kondo, M., et al., 2008. Cerebral white matter damage in frontotemporal dementia assessed by diffusion tensor tractography. Neuroradiology 50, 605–611.
Mori, S., Crain, B.J., Chacko, V.P., van Zijl, P.C., 1999. Three-dimensional tracking of axonal projections in the brain by magnetic resonance imaging. Ann. Neurol. 45, 265–269.
Mori, S., Oishi, K., Jiang, H., Jiang, L., Li, X., Akhter, K., et al., 2008. Stereotaxic white matter atlas based on diffusion tensor imaging in an ICBM template. NeuroImage 40, 570–582.
Peña-Salazar, C., Cendrós, P., Escoté, S., Romero, T., García-Barrionuevo, J., Roura-Poch, P., Arrufat, F., 2014. Capgras syndrome with left hemisphere neurological damage. J. Neuropsychiatry Clin. Neurosci. 26, E23–E24.
Philippi, C.L., Mehta, S., Grabowski, T., Adolphs, R., Rudrauf, D., 2009. Damage to association fiber tracts impairs recognition of the facial expression of emotion. J Neurosci. 29, 15089–15099.
Schwartzman, A., Dougherty, R.F., Lee, J., Ghahremani, D., Taylor, J.E., 2009. Empirical null and false discovery rate analysis in neuroimaging. NeuroImage 44, 71–82.
Silverstein, A.B., 1982. Two-and four-subtest short forms of the Wechsler adult intelligence scale-revised. J. Consult. Clin. Psychol. 50, 415–418.
Studholme, C., Hill, D., Hawkes, D.J., 1998. A normalized entropy measure of 3-D medical image alignment. Proc. Medical Imaging 1998 3338. SPIE Press, San Diego, CA, pp. 132–143.
Thiel, C.M., Studte, S., Hildebrandt, H., Huster, R., Weerda, R., 2014. When a loved one feels unfamiliar: a case study on the neural basis of Capgras delusion. Cortex 52, 75–85.
Thomas, C., Avidan, G., Jung, K.J., Behrmann, M., 2006. Disruption in structural connectivity in ventral cortex in congenital prosopagnosia. J. Vis. 6 (6), 88a Abstract 88.
Tranel, D., Damasio, A.R., 1985. Knowledge without awareness: an autonomic index of facial recognition by prosopagnosics. Science 228, 1453–1454.
Tranel, D., Fowles, D.C., Damasio, A.R., 1985. Electrodermal discrimination of familiar and unfamiliar faces: a methodology. Psychophysiology 22, 403–408.
Tranel, D.H., Damasio, H., Damasio, A.R., 1995. Double dissociation between overt and covert face recognition. J. Cogn. Neurosci. 7, 425–432.
Tzourio-Mazoyer, N., Landeau, B., Papathanassiou, D., Crivello, F., Etard, O., Delcroix, N., et al., 2002. Automated anatomical labeling of activations in SPM using a macroscopic anatomical parcellation of the MNI MRI single-subject brain. NeuroImage 15, 273–289.
Valdes-Sosa, M., Bobes, M.A., Quinones, I., Garcia, L., Valdes-Hernandez, P.A., Iturria, Y., et al., 2011. Covert face recognition without the fusiform-temporal pathways. NeuroImage 57, 1162–1176.
Wakana, S., Caprihan, A., Panzenboeck, M.M., Fallon, J.H., Perry, M., Gollub, R.L., et al., 2007. Reproducibility of quantitative tractography methods applied to cerebral white matter. NeuroImage 36, 630–644.
Wang, F., Kalmar, J.H., Edmiston, E., Chepenik, L.G., Bhagwagar, Z., Spencer, L., et al., 2008. Abnormal corpus callosum integrity in bipolar disorder: a diffusion tensor imaging study. Biol. Psychiatry 64, 730–733.
Watanabe, M., 1996. Reward expectancy in primate prefrontal neurons. Nature 382, 629–632.
Whitwell, J.L., Avula, R., Senjem, M.L., Kantarci, K., Weigand, S.D., Samikoglu, A., et al., 2010. Gray and white matter water diffusion in the syndromic variants of frontotemporal dementia. Neurology 74, 1279–1287.
Woodruff, P.W., McManus, I.C., David, A.S., 1995. Meta-analysis of corpus callosum size in schizophrenia. J. Neurol. Neurosurg. Psychiatry 58, 457–461.
Yendiki, A., Koldewyn, K., Kakunoori, S., Kanwisher, N., Fischl, B., 2013. Spurious group differences due to head motion in a diffusion MRI study. NeuroImage 88, 79–90.
Zhang, Y., Schuff, N., Du, A.T., Rosen, H.J., Kramer, J.H., Gorno-Tempini, M.L., et al., 2009. White matter damage in frontotemporal dementia and Alzheimer's disease measured by diffusion MRI. Brain 132, 2579–2592.